IEEE Robotics and Automation Letters (RA-L) paper, presented at ICRA 2023, London, UK. Cite as RA-L paper.

Advanced 2-DOF Counterbalance Mechanism based on Gear Units and Springs to Minimize Required Torques of Robot Arm

Hwi-su Kim[1], Jongwoo Park[1], Myeongsu Bae[2], Dongil Park[1], Chanhun Park[1], Hyun Min Do[1], *Member*, *IEEE*, Taeyong Choi[1], Doo-hyeong Kim[1] and Jinho Kyung[1]

***Abstract*—In recent years, human-robot cooperation has enhanced productivity and achieved high payload, speed, and accuracy. Integrating typical industrial robots in human-robot cooperation is challenging because their arms may cause serious injuries to humans during a collision due to malfunction or errors due to robot operators. Therefore, counterbalance robot arms that are capable of counterbalancing the gravitational torques due to the robot mass have been developed to decrease the required capacity of the motors and speeds of these robots. In this research, we propose an advanced counterbalance mechanism using gear units and springs to improve the durability and reliability compared to the previously proposed wire-based counterbalance mechanism, which is difficult to apply to a commercialized product because it can easily be broken or stretched when an excessive force is applied for a long period. Moreover, our proposed method was extended to a multi-DOF system using a parallelogram mechanism based on a timing belt and pulleys to achieve multi-DOF robotic arms. A 2-DOF counterbalanced arm was designed to verify the effectiveness of the proposed mechanism. The simulations and experimental results showed that the proposed mechanism effectively reduced the gravitational torques of each joint of the multi-DOF arm.**

***Index Terms* — Cooperating Robots, Robot Safety, gravity compensation, Counterbalance mechanism.**

I. Introduction

In recent years, with the increasing need for human-robot co-existence, various studies have been conducted to improve collision safety between humans and robots. The collaboration of high robotic performance (in terms of high payload, speed, and accuracy) with human intelligence (such as intuition or know-how) can improve the productivity in the industrial field; thus, more serviceable robots can interact with daily human activities in the near future [1-2].

Generally, the safety of a robot can be improved using active and passive methods. For active safety, collisions are predicted or measured using various sensors and the robot is controlled to avoid collision [3-4]. Specialized designed safety mechanisms can achieve the passive safety of robots. These devices may improve collision safety by decreasing the stiffness of the robot or absorbing the collision force [5-7]. However, this approach is not feasible because the performance of active safety strategies is limited owing to the sensing speed or range, control bandwidth, or human errors. In addition, the stiffness of the robot arm cannot be reduced enough to observe the collision force because it can lead to an inaccurate positioning of the robot arm; therefore, the safety mechanism is difficult to apply to commercial robots. Moreover, despite such safety strategies, the robots are still susceptible to causing collision danger since they are usually constructed with high-capacity components such as actuators, drivers, and gear reducers. Thus, robots are still a potential danger to humans.

To overcome the limitations of safety strategies, a counterbalance mechanism was suggested in a previous study [8-11]. The mechanism can minimize the capacity of the actuators or gear reducers to construct the robot arm by compensating the gravitational torque originating from the robot mass. Therefore, the robot requires relatively smaller torque delivered by relatively smaller capacity components. For industrial robots, a heavy counterweight is often used to balance the robot mass. However, this method cannot be used widely (in co-operation robot, service robot, etc.) because such a large and heavy external mass increases the total mass of robot which is closely related to inertial torque and battery power of mobile robots. To address these problems, several types of counterbalance mechanisms based on springs were developed in [8-12]. A multi-DOF counterbalance mechanism using a pseudo-parallelogram mechanism was suggested in [8], and a passive mechanical gravity compensator that is suitable for a variety of manipulator designs was developed using pulleys and tension springs in [9]. A 2-DOF counterbalance mechanism using gears, pulleys, and wires for low limb rehabilitation was developed and verified using computer simulations and actual equipment in [10], and a multi-DOF counterbalance robot arm

Manuscript received: December 14, 2021; Revised: March 3, 2022; Accepted: March 30, 2022.

This paper was recommended for publication by Editor Clement Gosselin upon evaluation of the Associate Editor and Reviewers' comments. This research was supported by a major project of the Korea Institute of Machinery and Materials (Project ID: NK238F).

[1]Hwi-Su Kim, Jongwoo Park, Dongil Park, Chanhun Park, Hyun Min Do, Taeyong Choi, Doo-hyeong Kim and Jinho Kyung is with the Korea Institute of Machinery & Materials, 156, Gajeongbuk - Ro, Yuseong - Gu, Daejeon 34103, Republic of Korea hskim81@kimm.re.kr

[2]Myeongsu Bae is with Dyence Tech, 36, Munjeong-ro 170beon-gil, Seo-gu, Daejeon, Republic of Korea bms1023@naver.com

Digital Object Identifier (DOI): see top of this page

using a spring, wire, and double parallelogram mechanism was developed in [11].

However, the application of previous counterbalance mechanisms to commercialized products is challenging because their durability and reliability are not guaranteed; these mechanisms include wires (or cables) for spring compression/ extension or constructing multi-DOF counterbalance mechanisms. Although wire based mechanisms have been widely used in robotic fields [18], they pose risks (safety, maintenance, etc..) and are vulnerable to breakage or stretching under excessive force for long duration. Therefore, they should be replaced by other durable and reliable mechanisms. To solve these problems, several types of non-wire based counterbalance mechanisms were suggested; however, mathematically, gravitational torque cannot be compensated completely in all postures. Therefore, complex optimization processes are required to minimize gravitational torque [12-14].

To address this, a concept model of the counterbalance mechanism based on gears and springs that can effectively, stably, and completely compensate for gravitational torque was suggested in the authors' previous article [17]. In this study, it was expanded to a multi-DOF system using the parallelogram mechanism based on timing belts and pulleys to provide the counterbalancing torque required at each joint and support the robot mass for the arm configuration. Therefore, the robot could be constructed with much smaller actuators and gear reducers than those of usual robots because the gravitational torques on each joint, which are usually greater than other factors composing the operational torque of the robot arm, were effectively compensated for by the suggested counterbalance mechanism while maintaining the desired performance (e.g., payload). Thus, collision safety, especially for static collision such as jamming, is improved with the human-robot co-existence or co-operation, since the forces applied on humans in dangerous situations, e.g., during collisions, are considerably reduced by using low-power actuators. (Note that dynamic collision primarily depends on the velocity and mass/inertia of a robot.) In addition, the energy consumption can be reduced; thus, reducing its operating costs. The practicality of the counterbalance mechanism was also improved by excluding a wire-driven mechanism from the design. In this study, prototype of 2-DOF counterbalance mechanism was designed & constructed, and feasibility was experimentally verified by measuring each joint torque of the arm with and without counterbalance mechanism.

The remainder of this paper is organized as follows. The operating principle and the structure of the multi-DOF counterbalance mechanism based on gears and springs are presented in Section II. The verification of the proposed mechanism using a designed 2-DOF counterbalance arm is described in Section III. In Section IV, we describe the various experiments conducted to verify the proposed mechanism and present the experimental results. Finally, the conclusion and future prospects are presented in Section V.

II. Design of Multi-DOF Counterbalance Mechanism Based on Gear Units

The equation of motion for a robot arm is

$$T = M(q)\ddot{q} + C(q,\dot{q})\dot{q} + g(q) \tag{1}$$

where $M(q)\ddot{q}$, $C(q, q)\dot{q}$, and $g(q)$ are the inertial torque, the Coriolis and centrifugal effects, and the gravitational torques, respectively. The Coriolis and centrifugal effects are not significant unless the robot moves at a high speed. The inertial torque, which accelerates or decelerates the robot, is usually small, provided that the co-operating robot moves at reasonable speeds and accelerations. Some gravitational torques result from the payload mass, but most of the gravitational torques stem from the robot mass, which is much greater than the payload mass for most robots. It is, therefore, established that counterbalancing the gravitational torques can minimize the torque required to operate the robot arm [8-12]. Moreover, previous works have proven that static balancing of robots can be effectively used not only for static but also for moderately dynamic operation [15-16].

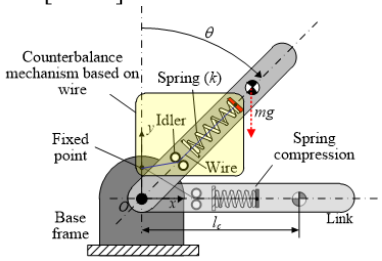

Fig. 1. Gravitational torque of 1-DOF arm

The gravitational torque T_g due to the mass of a simple 1-DOF robot, shown in Fig. 1, is given by

$$T_g = mgl_c \sin\theta \tag{2}$$

where m and l are the mass and length of the link, respectively, l_c is the distance from the joint axis to the link center of mass, and θ is the angular displacement of the link from the y-axis., This mechanism has limitations, as described in Section I. Thus, a durable and reliable mechanism should be used to generate a proper counterbalancing torque.

Therefore, in this research, a counterbalance mechanism based on gear units and springs was designed as a solution to overcome the limitations of previous mechanisms, as shown in Fig. 2.

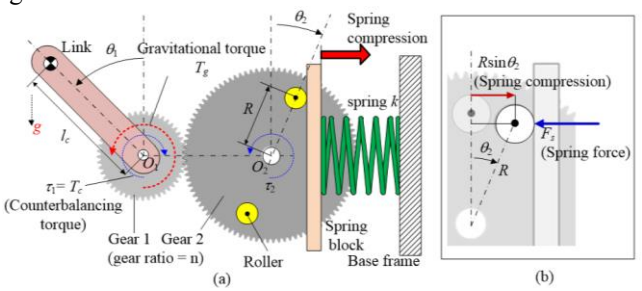

Fig. 2. Counterbalance mechanism based on spring and gear: (a) Concept model, and (b) detail view

A gear train with the proper gear ratio, compression springs, and rollers are used in the counterbalance mechanism to compensate for the gravitational torque of the robot. When the link is rotated, the spring is compressed by the spring block pushed by the roller fixed on gear 2, which is meshed with gear 1. Thus, a counterbalancing torque can be generated from the spring force and the moment arm R, whose length is the distance between the rotation center O_2 and the roller.

The relationship between the torques generated on gears 1 and 2 during rotation can be represented by

$$\tau_1 = \frac{1}{n}\tau_2 \tag{3}$$

where the gear ratio between gears 1 and 2 is n. When gear 2 is rotated by an angle θ_2 by the gear mesh, the spring is compressed to $R\sin\theta_2$ by the spring block pushed by the roller. Thus, the spring force F_s is applied to the roller, which can be expressed as follows:

$$F_s = kR\sin\theta_2 \tag{4}$$

where k is the spring stiffness. Therefore, the generated torques τ_1 and τ_2 can be calculated as

$$\begin{aligned}\tau_2 &= F_s R\cos\theta_2 \\ &= kR^2\sin\theta_2\cos\theta_2 \\ &= \frac{kR^2}{2}\sin(2\theta_2)\end{aligned} \tag{5}$$

$$\tau_1 = \frac{kR^2}{2n}\sin(2\theta_2) \tag{6}$$

When the generated torque on gear 1, τ_1, is represented as the counterbalancing torque T_c, the difference torque T_d can be computed as

$$T_d(\theta_1) = T_g(\theta_1) - T_c(\theta_1) \tag{7}$$

The gravitational torque T_g is canceled by the counterbalancing torque T_c to maintain the posture of the robot arm without any additional torque ($T_d = 0$). Therefore, from (2), (6), and (7), the relationship between the length l, a, and b, and the spring constant k can be described by

$$mgl\sin\theta_1 = \frac{kR^2}{2n}\sin(2\theta_2) \tag{8}$$

Therefore, if the gear ratio n is set to 2 ($\theta_1 = 2\theta_2$), the spring stiffness required to generate the appropriate counterbalancing torque can be selected based on the equation

$$k = 4mgl/R^2 \tag{9}$$

without the initial compression of the spring, unlike in previous counterbalance mechanisms based on wires and springs. (Note that minor compression is required in real world counterbalance mechanism design to maintain mechanical stability due to mechanical tolerance.)

The proposed counterbalance mechanism based on two gears (with a 1:2 gear ratio) is operated as shown in Figs. 3(a–d), while the link rotates from 0° to 180°. At the initial position, the counterbalancing torque is not generated, as the spring is not compressed while the gravitational torque is applied at the joint. The maximum gravitational torque is applied at the joint when the link is placed at 90°, and the spring force F_s and moment arm $R\cos\theta_1$ produce the maximum counterbalancing torque. Finally, when the link is positioned at 180°, there is no gravitational torque or counterbalancing torque because the moment arm is zero, even though the spring is fully compressed. It is also applied when the link is rotated from 180° to 360°, as shown in Fig. 3(e) and (f). (Note that it may require design to absorb the impact force between idler and spring block because impacts and noise can occur while contact is shifted from one idler to other with spring block, e.g., if a link is rotated from Fig. 3(b) to (f).)

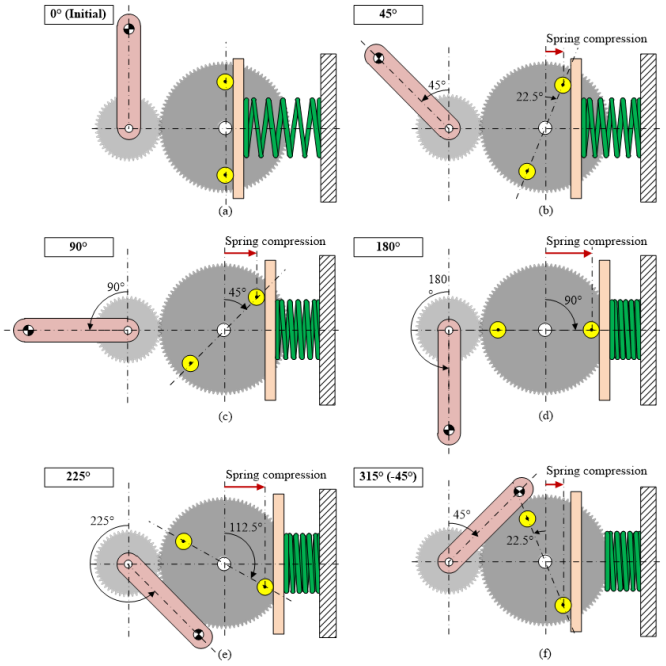

Fig. 3. Operation of counterbalance mechanism at θ equal (a) 0°, (b) 45°, (c) 90°, (d) 180°, (e) 225° (-135°), and (f) 315° (-45°)

Figure 4 shows the gravitational, counterbalancing, and difference torques as functions of the angular displacement θ_1 of the link when l_c = 500 mm, m = 10 kg, R_2 = 50 mm, and gravitational acceleration is approximately 9.81 m/s^2 as shown in Fig. 2. The required spring stiffness k = 78.48 N/mm can be calculated using Eq. (9). As shown in the simulation results, during the link rotation, a sinusoidal gravitational torque due to the mass of the link is applied to the joint, and it is completely compensated for by the counterbalancing torque generated from

the proposed counterbalance mechanism. Thus, no torque is generated to withstand the load owing to the weight of the link, but the link can maintain its posture. Therefore, with this counterbalance mechanism, the required torque and the capacity of the actuators used to construct the robot arm can be decreased significantly.

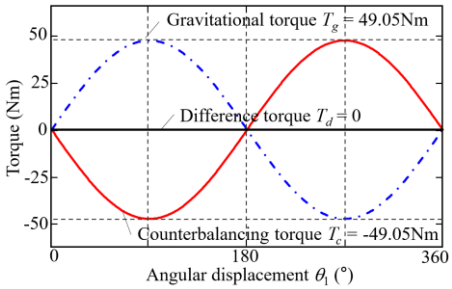

Fig. 4. Simulation results of a 1-DOF counterbalance mechanism based on gear unit and spring with given conditions

As mentioned in previous research, the counterbalance mechanism for a multi-DOF arm cannot be designed by merely placing a single-DOF counterbalance mechanism at each joint, because the torques required for each joint depend on the configuration of the other joint [11]. In this research, the proposed counterbalance mechanism was expanded to multi-DOFs for serial arms via a parallelogram mechanism using a timing belt and pulleys as an alternative solution to cables in previous studies. Moreover, in contrast to the previous counterbalance mechanism, the counterbalance mechanism for joint 2 in the proposed mechanism was placed on the base frame to reduce the weight of the rotational link and minimize the gravitational torque applied to joint 1. To this end, the timing pulley 2 fixed on link 2 was connected to the timing pulley 1, which was fixed on gear 2-1; thus, the rotation of link 2 could be delivered to the base frame. Therefore, the gravitational torque could be compensated by counterbalance mechanism 2 based on the angular displacement of joint 2, $\theta_{J1}+\theta_{J2}$, as shown in Fig. 5. It was noted that the counterbalance mechanisms for joints 1 and 2 were opposite to each other but on the same axis, as shown in Fig. 5.

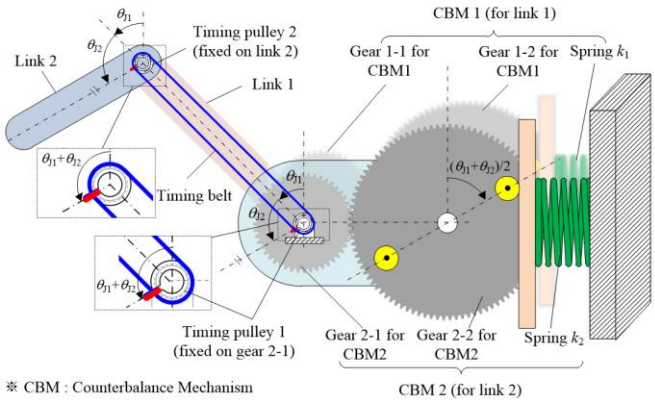

Fig. 5. Multi-DOF counterbalance mechanism based on parallelogram mechanism

The expected gravitational torques on each joint of the 2-DOF serial arm is given by

$$T_{g1}(\theta_{J1},\theta_{J2}) = (m_1 g l_{c1} + m_2 g l_1)\sin\theta_{J1} + m_2 g l_{c2}\sin(\theta_{J1}+\theta_{J2})$$
$$T_{g2}(\theta_{J1},\theta_{J2}) = m_2 g l_{c2}\sin(\theta_{J1}+\theta_{J2}) \quad (10)$$

where the subscripts denote the number of joints. Each counterbalancing torque is applied to each joint as follows:

$$Joint1: T_{d1}(\theta_{J1},\theta_{J2}) = T_{g1}(\theta_{J1},\theta_{J2}) - \{T_{c1}(\theta_{J1},\theta_{J2}) + T_{c2}(\theta_{J1},\theta_{J2})\}$$
$$Joint2: T_{d2}(\theta_{J1},\theta_{J2}) = T_{g2}(\theta_{J1},\theta_{J2}) - T_{c2}(\theta_{J1},\theta_{J2}) \quad (11)$$

where T_{dn} is the difference torque of the n^{th} joint required to maintain its posture [11]. Therefore, each counterbalance mechanism that can be designed to T_{d1} & T_{d2} is 0, for completely counterbalancing of the 2-DOF arm. Each spring stiffness, k_n, can be selected using Eq. (12). Figure 6 shows the operations of the designed 2-DOF counterbalance mechanism (CBM) based on the rotation of links 1 and 2.

$$k_1 = 4(m_1 g l_{c1} + m_2 g l_l)/{R_1}^2$$
$$k_2 = 4 m_2 g l_{c2}/{R_2}^2 \quad (12)$$

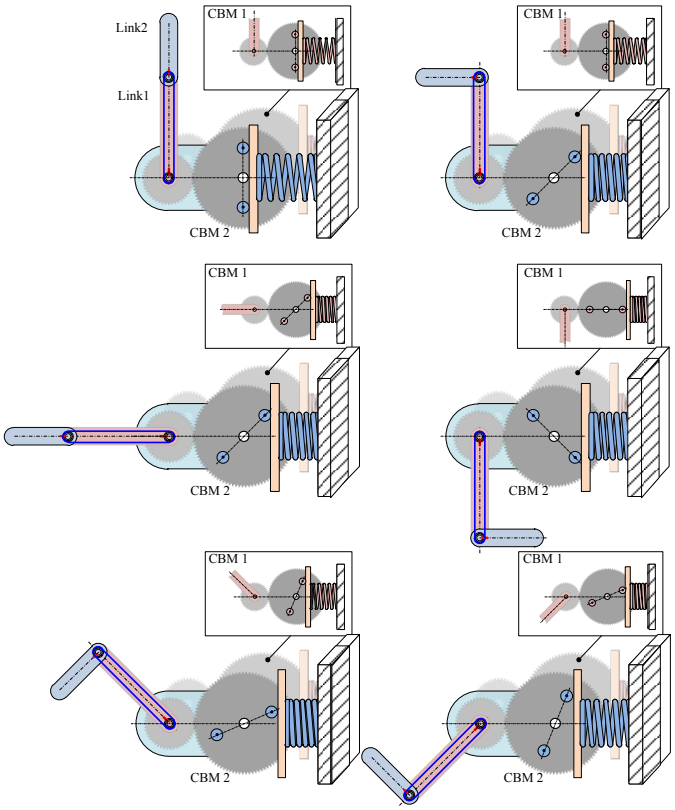

Fig. 6. Operation of 2 DOF counterbalance mechanism according to the rotation of links

III. Design of 2-DOF Counterbalance Arm

A 2-DOF (pitch – pitch joint) counterbalance arm was constructed to verify the performance of the proposed counterbalance mechanism, as shown in Fig. 7. Each design parameter was calculated using Eq. (12) to generate an appropriate counterbalancing torque for each joint in any of the

configurations of the 2-DOF serial arm.

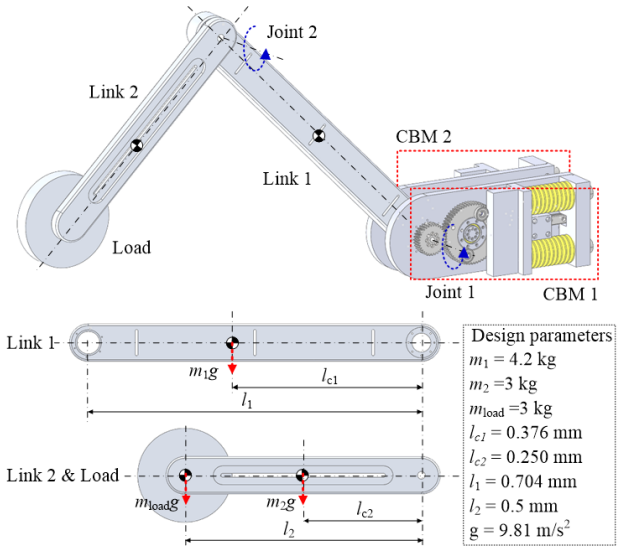

Fig. 7. Prototype design of a 2 DOF counterbalance arm with suggested counterbalance mechanism based on gear units and springs.

To construct CBM 1, we installed gear 1-1 on link 1 and connected it to gear 1-2 with a 1:2 gear ratio, as shown in Fig. 8. Rollers were placed on gear 1-2 with R_1 = 50 mm to push the spring block to compress the springs for generating the counterbalancing torque acting on joint 1. In this design, two springs were used for the required stiffness k_1 = 90.710 N/m, and linear guide units and spring shafts were used to prevent the spring block from buckling the springs during compression.

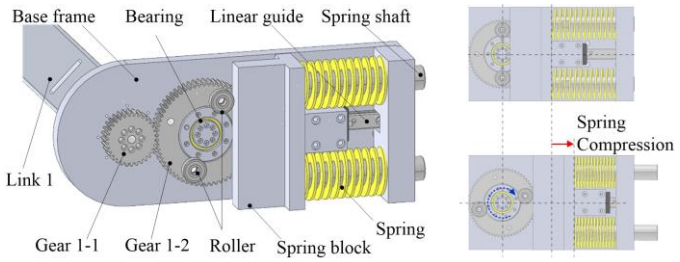

Fig. 8. Counterbalance mechanism for joint 1

As shown in Fig. 9, timing pulley 2 was installed on link 2 and connected to timing pulley 1 fixed on gear 2-1 using the timing belt to deliver the rotation of link 2 to CBM 2 placed on the base frame. Tension adjusters were applied on link 1 to maintain an appropriate tension of the timing belt. Gear 2-1 was also connected to gear 2-2 with a 1:2 gear ratio. Similar to the design of CBM 1, we placed rollers on gear 2-2 with R_2 = 46 mm and applied two springs for the required spring stiffness k_2 = 41.725 Nm for CBM 2. To evaluate the design of counterbalance mechanism with above parameters k_1, k_2, R_1, R_2 and others as shown in Fig. 7, several simulations were conducted in quasi-static condition.

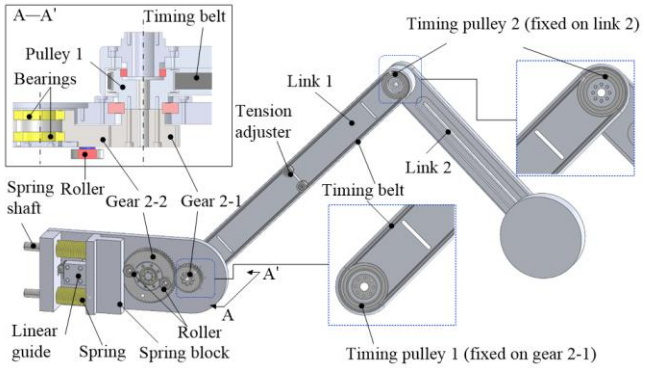

Fig. 9. Counterbalance mechanism for joint 2

The simulation results in Fig. 10 show that the gravitational torques applied on joints 1 and 2 were compensated with the designed counterbalance mechanism when joint 1 or joint 2 was rotated. Therefore, the torque required on each joint to maintain the arm's postures in any configuration was nearly 0 Nm; thus, the required capacity of the actuators can be considerably decreased to operate the serial arm. It was noted that a small difference between the gravitational and counterbalance torques resulted from the difference between the required calculated spring stiffness and the values of the selected commercial spring.

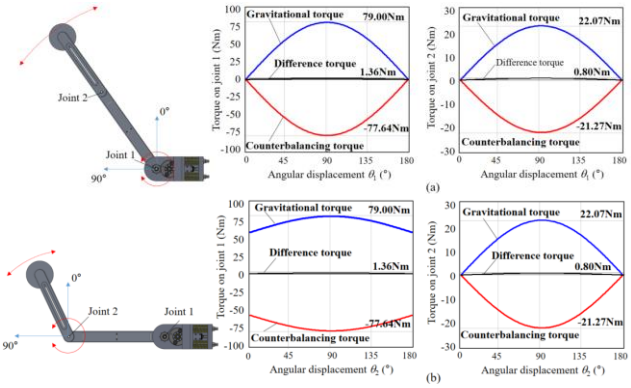

Fig. 10. Simulation results: gravitational torques, counterbalancing torque, and difference torque during rotation of (a) joint 1 and (b) joint 2.

IV. EXPERIMENTS

For the performance verification of the proposed counterbalance mechanism, an experimental setup with design parameters from Section III was constructed to measure the torque required to operate the 2 DOF serial arm, as shown in Fig. 11. It was noted that the springs that were much similar to the calculated value were selected among the commercial springs based on the required compressional length to prevent plastic deformation during the operations; therefore, small differences between the gravitational and counterbalancing torques were observed (CBM 1:45.1 N/m x 2ea and CBM 2:20.1 Nm x 2ea).

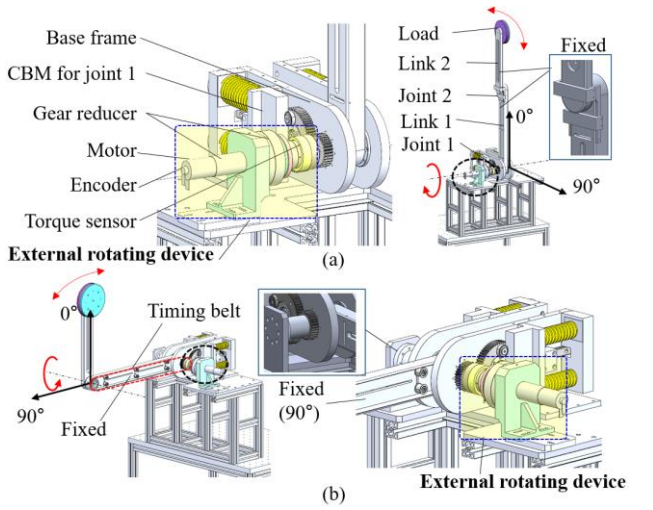

Fig. 11. Experimental setup to verify designed counterbalance mechanism for (a) joint 1 and (b) joint 2 of a serial arm.

Because there were no actuators in the constructed serial arm, an external rotating device was constructed to operate the arm and measure the torque applied on each joint during the rotation of the arm. The motor (capacity: 100 W, nominal torque: 0.2 Nm) and gear reducer (gear head type: 1:156, harmonic gear: 1:100) were selected to have sufficient torque to rotate the arm with and without the counterbalance mechanism, and a torque sensor (sensing range: 120 Nm, resolution: 1/80 Nm) was used as shown in Fig. 11(a). Link 1 of the serial arm was directly rotated by an external rotating device, which was installed on the base frame. In contrast, since gear 2-1, which is part of CBM 2, was connected to joint 2 with timing pulleys and belt, link 2 could be operated using an external rotating device installed on the base frame, as shown in Fig. 11(b). Link 2 was fixed with link 1, while link 1 was rotated. Subsequently, link 1 was fixed at 90° while joint 2 was rotated. Joint torques were measured by a torque sensor during each link and rotated from 0° to 180°. Note that each link was rotated gradually (< 2°/s) to minimize the dynamic effects such as acceleration or deceleration torques in this experiments.

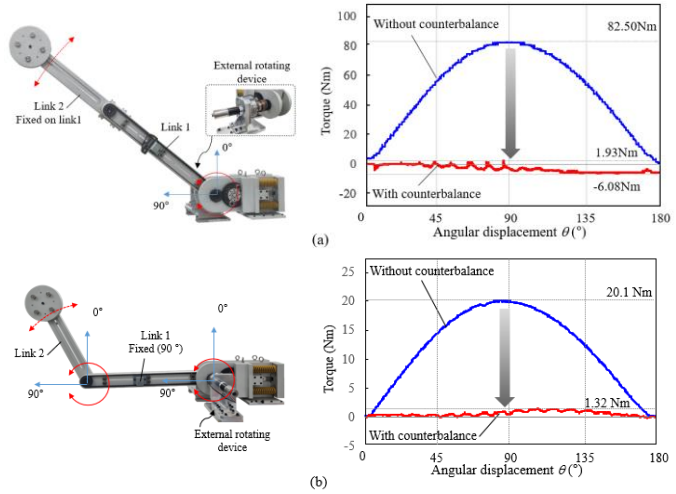

Fig. 12. Experimental result: measured torque of serial arm with and without counterbalance mechanism during rotation of (a) joint 1 and (b) joint 2.

As shown in the experimental results in Fig. 12, the maximum torques applied to joints 1 and 2 were 82.5 Nm and 20.1 Nm, respectively, while joints 1 and 2 of the serial arm rotated from 0° to 180°, without the counterbalance mechanism. However, with the developed counterbalance mechanism, the rotational torques of joints 1 and 2 significantly decreased to -6.08 ~ 1.93 Nm and 0 ~ 1.32 Nm, respectively. Moreover, the proposed mechanism generated an appropriate counterbalancing torque for each joint in the configuration. This means that only a small torque was required to operate the serial arm; therefore, the required capacity of the actuators and gear reducers could be minimized in constructing the robot arm. Small differences in the torques occurred, which might have been due to mechanical friction or difference between the calculated design parameters and the values of the selected commercial parts.

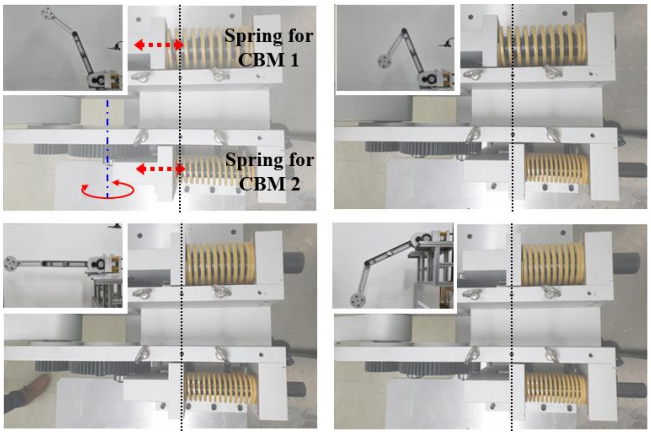

Fig. 13. Demonstration of static balancing of 2 DOF counterbalance arm and operation of counterbalance mechanism for joint 1 and joint 2.

Finally, the constructed counterbalance arm was operated manually to verify the performance of the proposed multi-DOF counterbalance mechanism. As shown in Fig. 13, counterbalance arm could maintain its posture in any configuration with combination of two counterbalance mechanism on each joint.

V. Conclusion

In this study, a counterbalance mechanism based on gear units and springs was proposed and extended to a multi-DOF system using a parallelogram mechanism based on the timing belt and pulleys. Moreover, a 2-DOF counterbalance arm was developed to verify the performance of the proposed mechanism. The following conclusions can be drawn from the results:

(1) The proposed counterbalance mechanism could compensate for the gravitational torques required to operate the robot arm and minimized the capacity of the actuators and gear reducers to improve collision safety between humans and robots.

(2) The proposed multi-DOF counterbalance mechanism was designed using gear units, springs, timing belts, and pulleys

without wires; advanced durability and reliability are expected for its applications in commercialized products in the real world.

REFERENCES

[1] H. Iwata and S. Sugano, "Design of human symbiotic robot TWENDY-ONE," *IEEE Int. Conf. on Robotics and Automation (ICRA)* 2009, pp. 580–586, 2009.

[2] Y. Sakagami, R. Watanabe, C. Aoyama, S. Matsunaga, N. Higaki, and K. Fujimura, "The intelligent ASIMO: system overview and integration," *IEEE/RSJ Int. Conf. on Intelligent Robots and Systems (IROS)* 2002, vol. 3, pp. 2478–2483, 2002.

[3] Morikawa, T. Senoo, A. Namiki, and M. Ishikawa, "Real-time collision avoidance using a robot manipulator with lightweight small high-speed vision systems," *Proc. IEEE Int. Conf. Robot. Automat.*, pp. 794–799, 2007.

[4] S. Haddadin, A. Albu-Schaffer, A. De Luca, and G. Hirzinger, "Collision detection and reaction: a contribution to safe physical human-robot interaction," *Proc. IEEE/RSJ Int. Conf. Intell. Robots Syst.*, pp. 3356–3363, 2008.

[5] B. S. Kim, J. B. Song, and J. J. Park, "A serial-type dual actuator unit with planetary gear train: basic design and applications," *IEEE/ASME Trans. Mechatron.*, vol. 15, no. 1, pp. 108–116, 2010.

[6] H. S. Kim, I. M. Kim, C. N. Cho, and J. B. Song, "Safe joint module for safe robot arm based on passive and active compliance," *Mechatronics*, Vol. 22, No. 7, pp. 1023–1030, 2012.

[7] G. Tonietti, R. Schiavi, and A. Bicchi, "Design and control of a variable stiffness actuator for safe and fast physical human/robot interaction," *Proc. IEEE Int. Conf. Robot. Automat.*, pp. 528–533, 2005.

[8] T. Morita, F. Kuribara, Y. Shiozawa, and S. Sugano, "A novel mechanism design for gravity compensation in three dimensional space," *IEEE/ASME Int. Conf. Adv. Intell. Mechatron*., pp. 163–168, 2003.

[9] N. Ulrich and V. Kumar, "Passive mechanical gravity compensation for robot manipulator," *IEEE Int. Conf. Robot. Automat.*, pp. 1536–1541, 1991.

[10] T. Nakayama, Y. Araki, and H. Fujimoto, "A new gravity compensation mechanism for lower limb rehabilitation," *IEEE Int. Conf. Mechatron. Automat.*, pp. 943–948, 2009.

[11] H. S. Kim and J. B. Song, "Multi-DOF counterbalance mechanism for a service robot arm," *IEEE/ASME Trans. Mechatron.*, vol. 19, no. 6, pp. 1756–1763, 2014.

[12] J. M. Herve, "Device for counter-balancing the forces due to gravity in a robot arm," U.S. Patent No. 4,620,829. 4, May 1986.

[13] V. L. Nguyen, C.-Y. Lin, and C.-H. Kuo, "Gravity compensation design of planar articulated robotic arms using the gear-spring modules," *J. Mech. Robot.*, vol. 12, no. 3, pp. 1–35, 2020.

[14] H.S. Kim, J. K. Min and J. B. Song, "Multiple-Degree-of Freedom Counterbalance Robot Arm Based on Slider-Crank Mechanism and Bevel Gear Unit*," IEEE. Trans. Robotics,* vol. 32, no. 1, 230-235, 2016.

[15] A. Martini, M. Troncossi, and A. Rivola, "Algorithm for the static balancing of serial and parallel mechanisms combining counterweights and springs: Generation, assessment and ranking of effective design variants," *Mech. Mach. Theory*, vol. 137, pp. 336–354, 2019.

[16] M. Carricato and C. Gosselin, "A statically balanced Gough/Stewart-type platform: Conception, design, and simulation," *J. Mech. Robot.*, vol. 1, no. 3, p. 031005, 2009.

[17] I. H. Kang, H. S. Kim, J.-B. Song, H. S. Lee, and I. S. Chang, "Manipulator equipped with counterbalance mechanism based on gear unit," *Trans. Korean Soc. Mech. Eng. A*, vol. 38, no. 3, pp. 289–294, 2014.

[18] A. Pott, "Cable-Driven Parallel Robot," *Theory and Application*, Spring, Cham, 2018.